Tanshinone IIA and Astragaloside IV promote the angiogenesis of mesenchymal stem cell-derived endothelial cell-like cells via upregulation of *Cx37*, *Cx40* and *Cx43*

ZHE LI[1,2*], SHA ZHANG[1*], LIANG CAO[1*], WEI LI[3], YU-CHEN YE[4], ZI-XUAN SHI[5], ZONG-REN WANG[1], LIAN-XU SUN[1], JIA-WEI WANG[1], LIN-TAO JIA[6] and WEN WANG[1]

[1]Department of Traditional Chinese Medicine, Xijing Hospital, Fourth Military Medical University, Xi'an, Shaanxi 710032; [2]Second Clinical Medical College, Shaanxi University of Traditional Chinese Medicine, Xianyang, Shaanxi 710026; Departments of [3]Histology and Embryology, and [4]Hepatobiliary Surgery, Xijing Hospital, Fourth Military Medical University, Xi'an, Shaanxi 710032; [5]Department of Acupuncture, Shaanxi Provincial Hospital of Traditional Chinese Medicine, Xi'an, Shaanxi 710003; [6]Department of Biochemistry and Molecular Biology, Fourth Military Medical University, Xi'an, Shaanxi 710032, P.R. China

Abstract. Tanshinone IIA (Tan IIA) and Astragaloside IV (AGS-IV) were used as therapeutic treatments for coronary heart diseases (CHDs) in ancient China. However, the underlying mechanisms mediating the effects of Tan IIA and AGS-IV in angiogenesis remain unknown. In the present study, mesenchymal stem cells (MSCs) were induced to differentiate into endothelial cell (EC)-like cells *in vitro* and the effects of Tan IIA and/or AGS-IV on the functions of these cells, including cell proliferation and tube formation, were assessed. Compared with the single-agent groups (Tan IIA or AGS-IV only), combined-agent (Tan IIA and AGS-IV) treatment significantly enhanced the proliferation and tube formation capacity of EC-like cells. In addition, the expression of connexin 37 (*Cx37*), *Cx40* and *Cx43* in the combined-agent group was significantly increased compared with the single-agent groups. Furthermore, enhanced gap junctional intercellular communication (GJIC) was identified in the combined-agent group, as evidenced by increased dye transfer in scrape-loading dye transfer assays. In conclusion, Tan IIA and AGS-IV may promote the angiogenesis of EC-like cells by upregulating the expression of *Cx37*, *Cx40* and *Cx43* and enhancing GJIC function. The results of the present study may provide experimental evidence for the clinical application of Tan IIA and AGS-IV as a treatment for CHDs.

Introduction

Cardiovascular diseases (CVDs) remain the leading cause of mortality in many developed and developing countries (1). Coronary heart diseases (CHDs), in particular myocardial infarction, are the most common cause of mortality among CVDs (1-3). The mortality rate of CVDs decreased by 30.8% from 2001 to 2011 in the US (4); however, the economic and social burdens of these diseases remain substantial. Furthermore, the mortality of CVDs increased by 14.9% in Iran (5) and 15% in China (6) between 1990 and 2010. With the fast pace of modern life, the morbidity rate in China is still increasing (7). There is therefore a need for novel CVD prevention and treatment methods.

Currently, the practice of mesenchymal stem cell (MSC) transplantation in CVDs is widely applied (8,9). Transplanted MSCs have been reported to develop into vascular cells to improve cardiac function in a rat model of dilated cardiomyopathy (10). There is also evidence that MSCs have potential beneficial effects in ameliorating CVDs in specific patients (11). MSCs may differentiate into mature cells (12) and exert physiological functions. Previous investigations have demonstrated that MSCs are able to differentiate into endothelial cells (ECs) *in vitro* (13,14). Tanshinone IIA (Tan IIA) and Astragaloside IV (AGS-IV) are extracted from *Salvia miltiorrhiza* and *Astragalus membranaceus,* respectively, which are traditional Chinese medicinal herbs (15). These compounds are able to accelerate the migration of MSCs towards the area of ischemic myocardium via upregulation of the CXCR4 pathway (16). In addition, stimulation with AGS-IV may promote the proliferation

Correspondence to: Professor Wen Wang, Department of Traditional Chinese Medicine, Xijing Hospital, Fourth Military Medical University, 169 Changle West Road, Xi'an, Shaanxi 710032, P.R. China
E-mail: jinzhou@fmmu.edu.cn

Professor Lin-Tao Jia, Department of Biochemistry and Molecular Biology, Fourth Military Medical University, 169 Changle West Road, Xi'an, Shaanxi 710032, P.R. China
E-mail: jialth@fmmu.edu.cn

*Contributed equally

and angiogenesis of human umbilical vein ECs (17). Similar effects on proliferation have also been demonstrated in endothelial progenitor cells following Tan IIA treatment (18). In general, these drugs are simultaneously used in the application of Traditional Chinese Medicine (15). However, whether these two compounds serve a synergistic role in treating CHDs with MSCs requires further experimental and clinical research.

Connexins are a family of structurally related transmembrane proteins that assemble to form gap junctions and connect the cytoplasm of adjacent cells (19). Molecules that flux through gap junctions constitute gap junctional intercellular communication (GJIC), which serves a crucial role in regulating metabolism (20,21), proliferation (22) and differentiation (23). Connexin 37 (*Cx*37) and *Cx*40 rely on one another for optimum expression in the vascular endothelium (24). Physiologically, *Cx*40 promotes the structural formation and function of blood vessels (25). The knockdown of *Cx*43 has been demonstrated to cause dysregulation in vasculogenesis (25-27). However, whether Tan IIA and AGS-IV affect the angiogenesis of MSC-derived EC-like cells via the regulation of connexins remains elusive.

In the present study, two drugs were combined to determine their effect on angiogenesis in MSC-derived EC-like cells compared with a single drug. It was investigated whether Tan IIA and AGS-IV affect the proliferation and angiogenesis of MSC-derived EC-like cells. Furthermore, differences in the expression profiles of *Cx*37, *Cx*40 and *Cx*43, as well as the function of GJIC, were examined to elucidate the underlying molecular mechanisms.

Materials and methods

Pharmacological agents. Tan IIA and AGS-IV (National Institutes for Food and Drug Control, Beijing, China; purity >98%) were dissolved in 0.1% dimethyl sulfoxide (DMSO) and were diluted to 0.2 and 0.4 μg/ml, respectively (16).

Isolation and culture of MSCs. The experimental protocols used in the present study were approved by the Ethics Committee of the Fourth Military Medical University (Xi'an, China). MSCs were isolated from the femurs and tibias of 10 Sprague Dawley rats (4-7 days old; ~20 g; 5 males and 5 females; bred in standard specific-pathogen-free conditions with food and water provided *ad libitum,* in the Animal Facility of the Fourth Military Medical University) and were subsequently suspended in Dulbecco's Modified Eagle Medium Nutrient Mixture F-12 (Gibco; Thermo Fisher Scientific, Inc., Waltham, MA, USA) supplemented with 12% FBS. Cells were isolated and cultured as previously described (28,29) with minor modifications. Briefly, the cells were seeded into 25 cm^2 flasks (Corning Incorporated, Corning, NY, USA) and incubated at 37˚C for 48 h in an atmosphere containing 5% CO$_2$. MSCs at their third passage were used in the following experiments. Briefly, MSCs were incubated with anti-CD34-FITC (Thermo Fisher Scientific, Inc.; no. 11-0341-81), anti-CD44-FITC (Thermo Fisher Scientific, Inc.; no. 11-0441-82), anti-CD45-FITC (Thermo Fisher Scientific, Inc.; no. 11-0452-82), anti-CD29-FITC (Thermo Fisher Scientific, Inc.; no. 11-0291-82), anti-CD90-FITC (Thermo Fisher Scientific, Inc.; no. 11-0900-81) or corresponding IgG

(Thermo Fisher Scientific, Inc.; no. 11-4614-80). All antibodies were used at a final dilution of 1:100. Cells were incubated with the primary antibodies at 4˚C for 30 min. Necrotic cells were excluded via 1 μl propidium iodide (PI) staining at room temperature for 30 min. A FACSCalibur flow cytometer (BD Biosciences, San Jose, CA, USA) and EXP032-ADC analysis software (Beckman Coulter, Brea, CA, USA) were used for the subsequent analysis.

Induction of EC-like cells. MSCs were cultured in Dulbecco's modified Eagle's medium (Hyclone; GE Healthcare Life Sciences, Logan, UT, USA) supplemented with 10 ng/ml vascular endothelial growth factor (VEGF; SinoBiological, Inc., Beijing, China) and 2 ng/ml basic fibroblast growth factor (bFGF; SinoBiological, Inc.) (30) at 37˚C for 14 days. The medium was replaced every 3-4 days and the cellular morphology was observed under a light microscope at x200 magnification.

Immunohistochemistry assay. To validate the EC-like cells, Factor VIII expression was assessed using an immunohistochemistry assay as previously described (31). Cells were fixed using 4% paraformaldehyde for 20 min at room temperature, treated with 0.3% H$_2$O$_2$ for 5 min at room temperature, permeabilized using 0.5% Triton X-100 and blocked using goat serum (Beyotime Institute of Biotechnology, Haimen, China) for 10 min at room temperature. The cells were incubated with rabbit anti-Factor VIII (1:200; BIOSS, Beijing, China; no. bs-0434R) for 4 h at 37˚C. Following incubation with biotinylated goat anti rabbit IgG (1:200; Wuhan Boster Biological Technology, Ltd., Wuhan, China; BA1006) for 30 min at room temperature, the cells were treated with a streptavidin-biotin complex for 20 min at 37˚C. The final immunoreactions were conducted using 3,3'-Diaminobenzidine for 5 min at room temperature according to the manufacturer's protocol (Wuhan Boster Biological Technology, Ltd.). Finally, the slides were mounted with neutral balsam (Origene Technologies, Inc., Beijing, China) and observed under an inverted microscope at x200 magnification (Olympus Corp., Tokyo, Japan).

Cell cycle analysis. Following fixation with ethanol overnight at 4˚C, the cells were treated with RNA enzyme (50 μg/ml; Abcam, Cambridge, MA, USA; ab14085) at 37˚C for 30 min, followed by PI (100 μg/ml; Abcam; no. ab14085) on ice for 30 min. The fluorescence intensities were determined using a flow cytometer (BD Biosciences) and MultiCycle analysis software (Beckman Coulter).

MTT assay. Cells at 60% confluence (3x10^3/well) were seeded in 96-well plates and treated with Tan IIA (0.2 μg/ml), AGS-IV (0.2 μg/ml) or Tan IIA + AGS-IV for 24, 48 or 72 h. A total of 20 μl 0.5% MTT solution (Sigma Aldrich; Merck KGaA, Darmstadt, Germany) was added and incubated for 4 h at 37˚C. Formazan crystals were produced and dissolved in 150 μl of DMSO. The spectrophotometric absorbance was measured using a 168-1000XC microtiter plate reader (Bio-Rad Laboratories, Inc., Hercules, CA, USA) at 490 nm. Each assay was repeated three times with three wells per experimental condition.

In vitro tube formation assay. A total of 50 μl Matrigel matrix (BD Biosciences,) was applied to each well of a 96-well plate
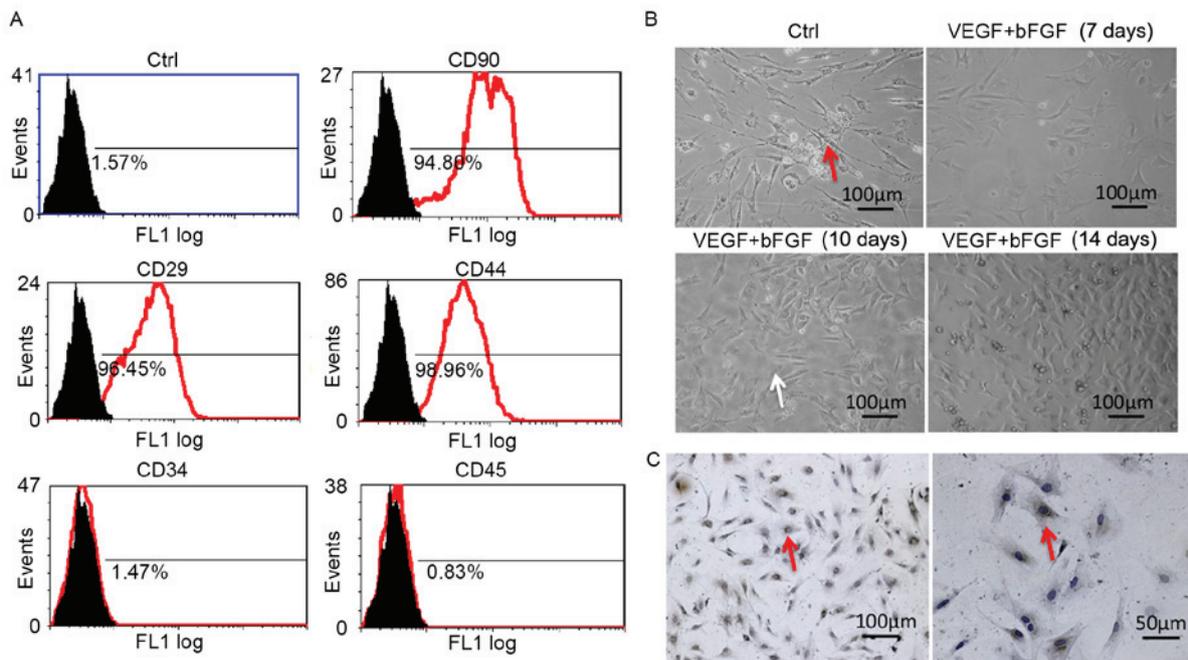
Figure 1. VEGF and bFGF promote the differentiation of MSCs into EC-like cells. (A) Expression of MSC surface markers was confirmed using flow cytometry. (B) Morphological features of isolated MSCs and MSC-derived EC-like cells following induction as observed under an inverted microscope. The red and white arrows indicate spindle-shaped and polygon-shaped cells, respectively. Magnification, x20. (C) Factor VIII expression was detected in MSC-derived EC-like cells via immunohistochemistry and light microscopy with brown staining indicating the positive signal. VEGF, vascular endothelial growth factor; bFGF, basic fibroblast growth factor; MSCs, mesenchymal stem cells; EC, endothelial cell; Ctrl, control; CD, cluster of differentiation.

and solidified at 37˚C for 2 h. A total of 100 μl complete medium was subsequently added to EC-like cells (5x10^4 cells/well) and incubated at 37˚C in an atmosphere containing 5% CO_2 for 6 h. Each treatment was performed for 3 wells. The 96-well plates were gently shaken and incubated at 37˚C for 48 h, and then observed under an inverted microscope at x200 magnification.

Reverse transcription-quantitative polymerase chain reaction (RT-qPCR). Total RNA was extracted from induced EC-like cells using TRIzol reagent (Invitrogen; Thermo Fisher Scientific, Inc.) according to the manufacturer's protocol. cDNA was synthesized from the total RNA using an RT kit following the manufacturer's protocol (Beijing TransGen Biotech Co., Ltd.). qPCR was performed using a SYBR Premix EX Taq kit following the manufacturer's protocol (Takara Biotechnology Co., Ltd., Dalian, China) with β-actin as an internal control. The final volume was 10 μl, containing 1 μl forward primer and 1 μl of reverse primer. PCR products were measured using the CFX96 Real-Time RT-PCR detection system (Bio-Rad Laboratories, Inc.), and the relative gene expression was calculated using the $2^{-\Delta\Delta Cq}$ method (32) using CFX96 Manager Software v2.0 (Bio-Rad Laboratories, Inc.). Thermocycling conditions were as follows: Initial denaturation at 95˚C for 30 sec, followed by 40 cycles of 95˚C for 5 sec, 60˚C for 30 sec and 72˚C for 15 sec. The primers used for RT-qPCR were as follows: *Cx*37, forward 5'-CCTTGTGCATCTCCAGGTCC-3' and reverse 5'-GAAGACCACCAGCACAGTGA-3'; *Cx*40, forward 5'-AAAGGAAGCCAGAAGGCTCGG-3' and reverse 5'-CCGATGACTGTGGAGTGCTT-3'; *Cx*43, forward 5'-TGAGGGAAGTACCCAACAGC-3' and reverse 5'-TCTGGGCACCTCTCTTTCACT-3'; β-actin, forward 5'-ACCACAGGCATTGTTCTGGA-3' and reverse 5'-AGGGCGACGTAACACAGTTT-3'.

Western blotting. Total proteins were extracted from each group by lysing the cells with RIPA lysis buffer (Beyotime Institute of Biotechnology) and protein quantification was performed using a bicinchoninic acid assay. Proteins were separated by 12% SDS-PAGE and were electroblotted onto a nitrocellulose filter membrane. The membranes were subsequently blocked with 5% skim milk for 1 h at room temperature and incubated with rabbit anti-rat *Cx*37 (1:400; Invitrogen; Thermo Fisher Scientific, Inc; no. 40-4300), rabbit anti-rat *Cx*40 (1:1,000; Abcam; no. ab183648), rabbit anti-rat *Cx*43 (1:1,000; Cell Signaling Technology, Danvers, MA, USA; no. 3512) and anti-tubulin (1:2,000; HuaBio, Hangzhou, China; no. EM0103) antibodies overnight at 4˚C, followed by incubation with IRDye 800™ goat anti-rabbit IgG (1:15,000; Rockland, Inc., Limerick, PA, USA; no. 611-132-122) at room temperature for 2 h. The final visualization of the blots was performed using an Odyssey infrared scanning system (LI-COR Biosciences, Lincoln, NE, USA), followed by quantification via the integration of the optical density value of each band with Gel-Pro analyzer 4.0 software (Media Cybernetics, Inc., Rockville, MD, USA) and GraphPad Prism 5.0 software (GraphPad Software, Inc., La Jolla, CA, USA).

Scrape-loading dye transfer experiment. Scrape-loading dye transfer experiments were used to detect the function of the GJIC as previously described (33). In brief, the cells were washed three times with PBS. A sterile scalpel blade was subsequently used to generate multiple scratches through the cell monolayer in the presence of PBS containing 1 mg/ml Lucifer yellow (Thermo Fisher Scientific, Inc.). The cells were incubated at 37˚C for 20 min, rinsed with PBS
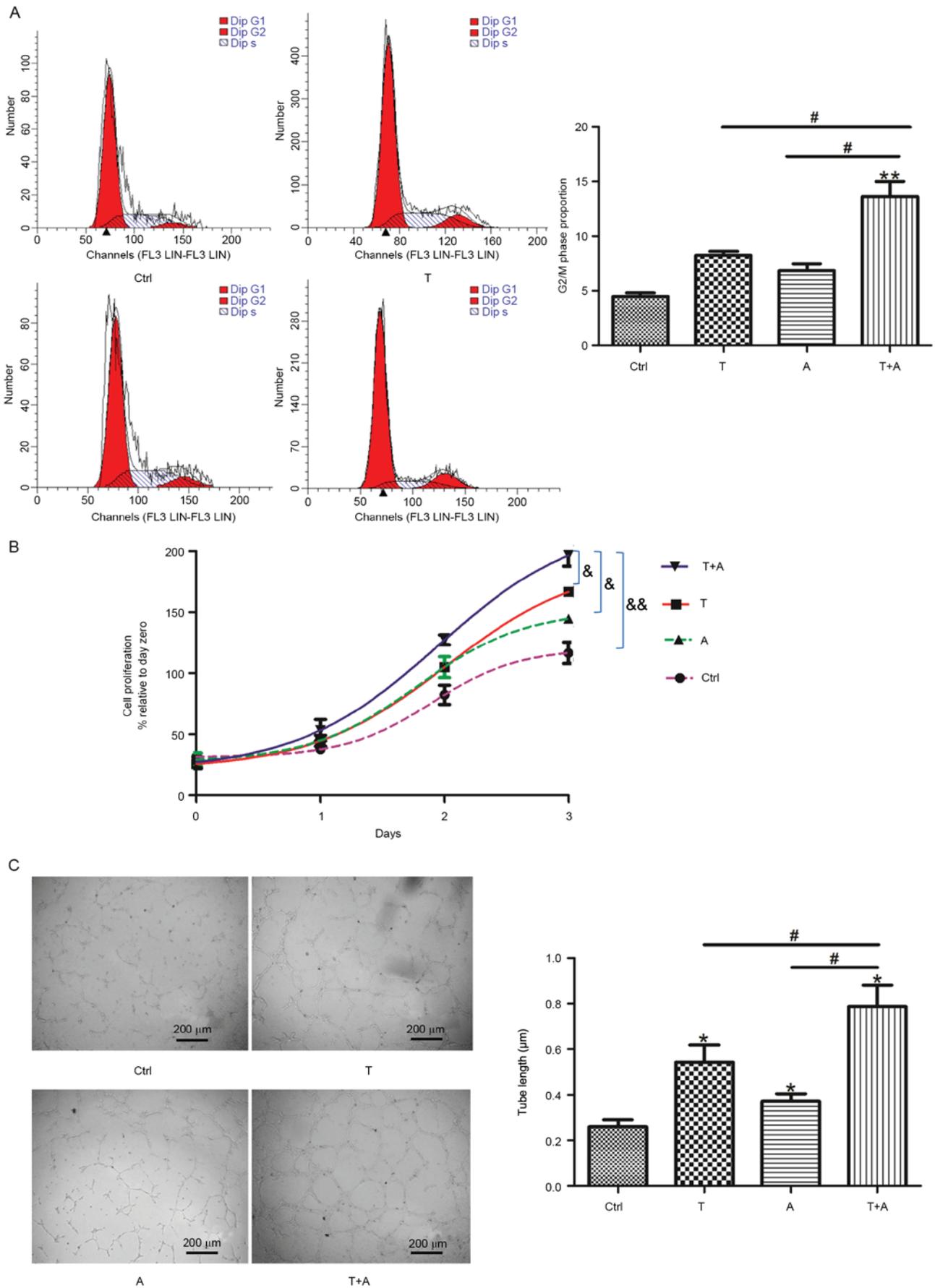
Figure 2. Treatment with T and A promotes proliferation and angiogenesis of mesenchymal stem cell-derived endothelial cell-like cells. Following treatment with T (0.2 µg/ml), A (0.4 µg/ml) or T+A for 72 h, (A) cell cycle distribution was assessed using flow cytometry, (B) cell proliferation was assayed via MTT and (C) angiogenesis was assessed via tube formation assays. n=4. *P<0.05 and **P<0.01 vs. Ctrl group. #P<0.05 vs. T+A group. &P<0.05; &&P<0.01. T, Tanshinone IIA; A, Astragaloside IV; Ctrl, control.
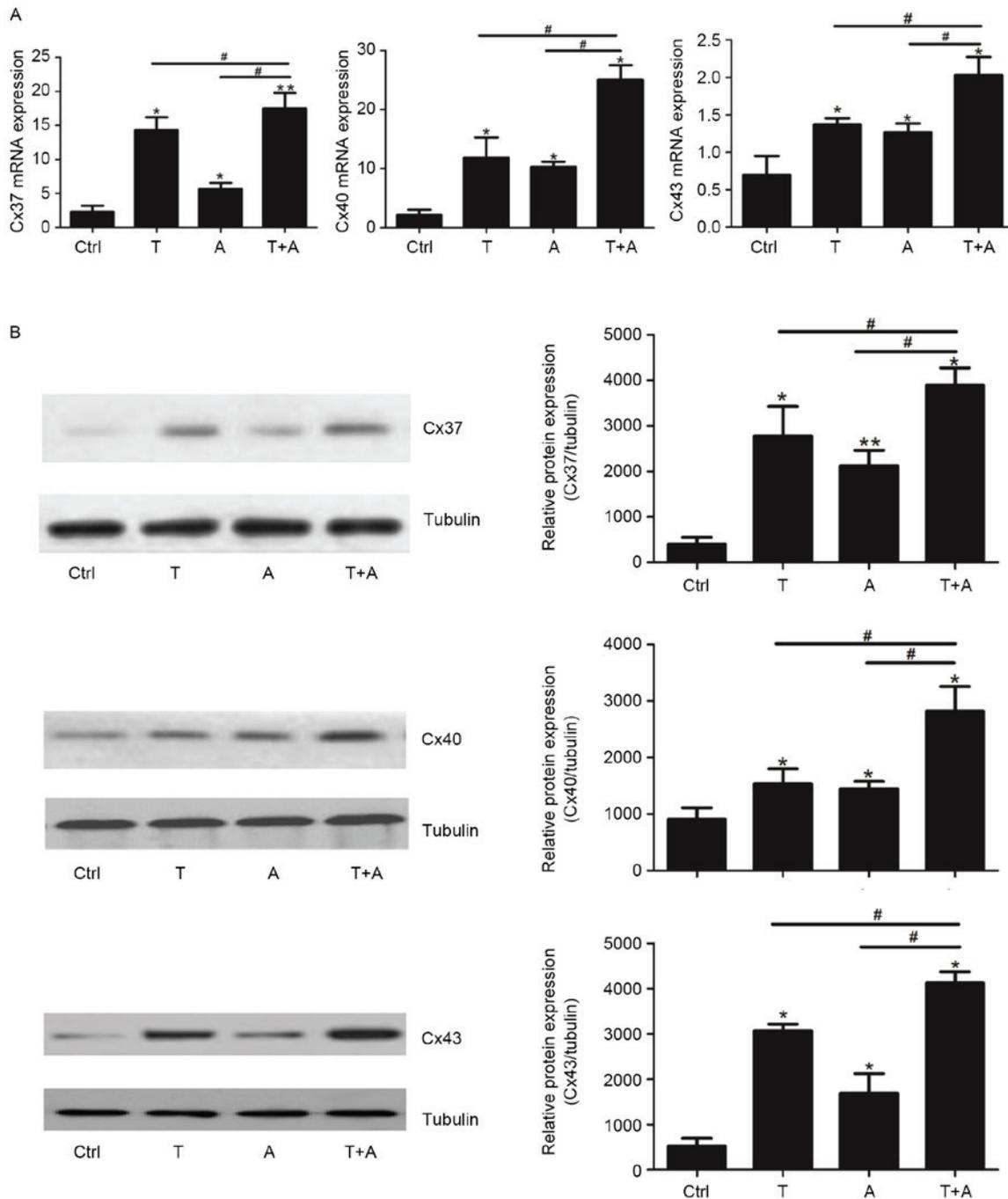
Figure 3. T and A upregulate *Cx*37, *Cx*40, and *Cx*43 expression in mesenchymal stem cell-derived endothelial cell-like cells. Following treatment with T, A or T+A for 72 h, the (A) mRNA and (B) protein levels of *Cx*37, *Cx*40, and *Cx*43 were assessed using reverse transcription-quantitative polymerase chain reaction and western blotting, respectively. *$P<0.05$ and **$P<0.01$ vs. Ctrl group. #$P<0.05$ vs. T+A group. T, Tanshinone IIA; A, Astragaloside IV; *Cx*, connexin; Ctrl, control.

and immediately fixed with 4% paraformaldehyde at room temperature for 20 min. The diffusion distance of dyes was determined by measuring the longest distance of diffusion perpendicular to the scrape using Image Pro Plus 6.0 (Media Cybernetics, Inc.).

Statistical analysis. SPSS 19.0 (IBM Corp., Armonk, NY, USA) was used for statistical analysis and all data are presented as the mean ± standard deviation For two-group comparisons and multiple group comparisons, Student's t-test and one-way analysis of variance with Dunnett's post-hoc test was used,

respectively. $P<0.05$ was considered to indicate a statistically significant difference.

Results

VEGF and bFGF promote the differentiation of MSCs into EC-like cells. The expression levels of CD90, CD45, CD44, CD29 and CD34 in third generation MSCs were analyzed using flow cytometry. Of these surface markers, the expression of CD44, CD29 and CD90 was positive (Fig. 1A), which suggests the presence of MSC characteristics. However, the
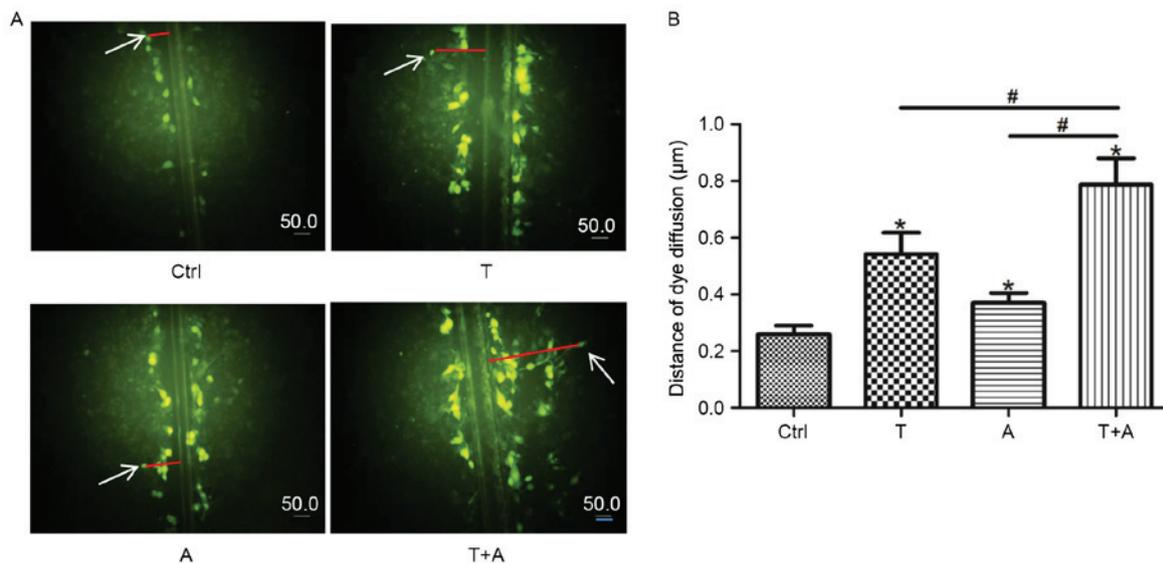
Figure 4. Treatment with T and A promotes GJIC functions mesenchymal stem cell-derived endothelial cell-like cells. (A) GJIC was evaluated 20 min following the scrape and incubation with fluorescent dye. (B) The distance that dye diffused perpendicular to the scrape was measured and calculated. *P<0.05 vs. Ctrl group. #P<0.05 vs. T+A group. T, Tanshinone IIA; A, Astragaloside IV; GJIC, gap junctional intercellular communication; *Cx*, connexin; Ctrl, control.

expression of CD34 and CD45 was negative (Fig. 1A), which indicates that there was no contamination of hematopoietic cell lineages.

The morphological features of MSCs were also characterized. Prior to stimulation, MSCs exhibited a long spindle shape and aggregative growth (Fig. 1B). MSCs induced using VEGF and bFGF exhibited progressive changes (Fig. 1B); on day 7, cells became shorter; on day 10, a portion of the cells became polygonal; by day 14, the majority of cells were polygonal. Factor VIII was expressed in the cells by day 14 following induction, as evidenced by the immunohistochemistry assay (Fig. 1C), which suggests that these cells were EC-like.

Treatment with Tan IIA and AGS-IV promotes proliferation and tube formation in induced MSCs. Following the identification of EC-like cells, the proliferation and tube formation of these cells was investigated. First, the effects of Tan IIA, AGS-IV and a combination of the two on proliferation of MSC-derived EC-like cells were assessed. Following Tan IIA and/or AGS-IV stimulation, the proportion of cells in S phase was increased compared with the control group (Fig. 2A). Furthermore, compared with the AGS-IV-treated group, a increase in the percentage of cells in the S phase was identified in the combined-agent group. The change in the proportion of cells in the G2/M phase was not significant in the single-agent group compared with the control group; however, it was significantly increased in the combined-agent group compared with cells treated with AGS-IV or Tan IIA alone (P<0.05; Fig. 2A). The MTT assay demonstrated that cell proliferation ability was significantly higher in the combined-agent group compared with all groups (P<0.05; Fig. 2B). These results suggest that Tan IIA and AGS-IV may promote the proliferation of induced MSCs. The capacity of angiogenesis was assessed using tube formation assays, which indicated that the tubular structural integrity was better in the combined-agent group compared with single-agent groups, and the tube length of the former group was thicker (P<0.05; Fig. 2C).

Treatment with Tan IIA and AGS-IV promotes Cx37, Cx40 and Cx43 expression in induced MSCs. The gap junction proteins *Cx*37, *Cx*40 and *Cx*43 are expressed by ECs, to regulate the vascular functions associated with angiogenesis and vascular remodeling (26,34). The expression levels of *Cx*37, *Cx*40 and *Cx*43 mRNA and protein were assessed following single- or combined-agent treatment. The expression of *Cx*37, *Cx*40 and *Cx*43 mRNA was significantly upregulated in the single-agent and combined-agent groups compared with the control group (P<0.05; Fig. 3A). Treatment with Tan IIA and AGS-IV combined induced a significantly greater increase in *Cx*37, *Cx*40 and *Cx*43 expression compared with either agent alone (P<0.05; Fig. 3A. The expression of *Cx*37, *Cx*40 and *Cx*43 protein among the different groups was similar to the pattern observed with mRNA expression; the expression of all proteins was significantly increased in the single- and combined-agent treatment groups compared with the control group (P<0.05; Fig. 3B) However, this effect was significantly greater in the combined-agent group compared with the single-agent group for *Cx*37, *Cx*40 and *Cx*43 protein expression (P<0.05; Fig. 3B).

Treatment with Tan IIA and AGS-IV promotes GJIC functions in induced MSCs. Following the assessment of connexin expression levels, the functions of GJIC were further assessed via a scrape-loading dye transfer experiment. At 20 min following the scrape and incubation with Lucifer yellow, the fluorescent-positive cell area was detected. The fluorescent dye was present only in the first layer of cells in the control group, whereas it was transferred to the second and third layer of cells adjacent to scratches in the single-agent group (P<0.05; Fig. 4A and B). Furthermore, a significantly greater increase in transfer distance was identified in the combined-agent group compared with the single-agent groups (P<0.05; Fig. 4A and B). These findings indicate that the combination of Tan IIA and AGS-IV may promote GJIC functions significantly more than treatment with either agent alone.

Discussion

In recent years, stem cell therapy has become an important strategy used to address irreversible damage to myocardial cells (35). The mechanisms involved in stem cell therapy include (36): i) Cardiac regeneration; MSCs may not only differentiate into cardiomyocytes, which replace infarcted myocardial cells, repair damaged tissue and improve cardiac function, but may also differentiate into EC and smooth muscle cells, which improves myocardial ischemia (37). ii) Cardiac repair; MSCs are associated with the regulation of angiogenesis, the proliferation of cardiomyocytes and the recruitment of resident cardiac stem cells via the secretion of cytokines and growth factors (38). iii) Niche contribution and cardiac remodel regulation have also been reported to participate in cell therapy for CHDs (36).

A previous study by our group demonstrated that the combination of Yiqi Huoxue Qidantongmai tablet (QDTMT) and MSC transplantation promoted MSCs to differentiate into EC-like cells, which increased the microvascular density of the ischemic area (39). The present study was designed to further investigate the effects of Tan IIA and AGS-IV, the active components of QDTMT, on the function of EC-like cells derived from MSCs, as well as the potential underlying molecular mechanisms thereof. MSCs were separated and cultured as previously described (40) and characterized via flow analysis. Cytokines were added to induce the differentiation of MSCs into EC-like cells, which resemble ECs in morphology and immunohistochemistry. The effects of the Tan IIA and AGS-IV on the function of EC-like cells were investigated via the detection of cell proliferation and tube formation. Compared with the single-agent group, the combined-agent group significantly improved the tube formation capacity and proliferation ability of EC-like cells, which suggests that the combination of Tan IIA and AGS-IV is more beneficial for angiogenesis compared with either drug alone. As previously reported, the cellular behaviors of ECs in the processes of vessel formation, including cell survival, migration and vascularization, are associated with GJIC (41). Deficiencies in $Cx37$, $Cx40$ or $Cx43$, which constitute the structural units of GJIC, may lead to abnormal vascular development (24,26,42). In the present study, levels of $Cx37$, $Cx40$ and $Cx43$ were upregulated more in the combined-agent group compared with the single-agent group. Scrape-loading dye transfer experiments further demonstrated that GJIC function was improved in the combined-agent group. Such changes in gap junctions may explain the improved proliferation and tube formation observed in the combined-agent group. These findings have the potential to provide a preliminary experimental basis for the combined use of traditional drugs in cell therapy for CHDs to promote blood supply reconstruction.

To fully elucidate the association between expression levels of $Cx37$, $Cx40$ and $Cx43$ and GJIC function, further investigation using inhibitors or genetic interference is required. In microvessels, the recruitment of pericytes by ECs is a symbolic event of vascular maturation (43). However, it remains unknown whether the Chinese herbs YiQi and HuoXue promote blood perfusion and eventually improve the repair of myocardial ischemia injury by recruiting pericytes and regulating pericyte differentiation.

In conclusion, combined treatment with Tan IIA and AGS-IV may contribute to the promotion of angiogenesis by upregulating $Cx37$, $Cx40$ and $Cx43$ expression and improving GJIC function. However, whether the experimental outcome identified in rat-derived cells may also be applied to humans remains unclear. Additional *in vivo* and *in vitro* experiments are required to determine whether the combination of Tan IIA and AGS-IV may be applied to increase the therapeutic efficacy of stem cell therapy for CHDs.

Acknowledgements

References

1. Huang CK, Lee SO, Chang E, Pang H and Chang C: Androgen receptor (AR) in cardiovascular diseases. J Endocrinol 229: R1-R16, 2016.
2. Carlsson AC, Li X, Holzmann MJ, Wändell P, Gasevic D, Sundquist J and Sundquist K: Neighbourhood socioeconomic status and coronary heart disease in individuals between 40 and 50 years. Heart 120: 775-782, 2016.
3. Gaziano TA, Bitton A, Anand S, Abrahams-Gessel S and Murphy A: Growing epidemic of coronary heart disease in low- and middle-income countries. Curr Probl Cardiol 35: 72-115, 2010.
4. Mozaffarian D, Benjamin EJ, Go AS, Arnett DK, Blaha MJ, Cushman M, de Ferranti S, Després JP, Fullerton HJ, Howard VJ, *et al*: Heart disease and stroke statistics-2015 update: A report from the American Heart Association. Circulation 131: e29-e322, 2015.
5. Forouzanfar MH, Sepanlou SG, Shahraz S, Dicker D, Naghavi P, Pourmalek F, Mokdad A, Lozano R, Vos T, Asadi-Lari M, *et al*: Evaluating causes of death and morbidity in Iran, global burden of diseases, injuries, and risk factors study 2010. Arch Iran Med 17: 304-320, 2014.
6. Yang G, Wang Y, Zeng Y, Gao GF, Liang X, Zhou M, Wan X, Yu S, Jiang Y, Naghavi M, *et al*: Rapid health transition in China, 1990-2010: Findings from the global burden of disease study 2010. Lancet 381: 1987-2015, 2013.
7. Jiang L, Krumholz HM, Li X, Li J and Hu S: Achieving best outcomes for patients with cardiovascular disease in China by enhancing the quality of medical care and establishing a learning health-care system. Lancet 386: 1493-1505, 2015.
8. Segers VF and Lee RT: Stem-cell therapy for cardiac disease. Nature 451: 937-942, 2008.
9. Han D, Huang W, Li X, Gao L, Su T, Li X, Ma S, Liu T, Li C, Chen J, *et al*: Melatonin facilitates adipose-derived mesenchymal stem cells to repair the murine infarcted heart via the SIRT1 signaling pathway. J Pineal Res 60: 178-192, 2016.
10. Nagaya N, Kangawa K, Itoh T, Iwase T, Murakami S, Miyahara Y, Fujii T, Uematsu M, Ohgushi H, Yamagishi M, *et al*: Transplantation of mesenchymal stem cells improves cardiac function in a rat model of dilated cardiomyopathy. Circulation 112: 1128-1135, 2005.
11. Burt RK, Loh Y, Pearce W, Beohar N, Barr WG, Craig R, Wen Y, Rapp JA and Kessler J: Clinical applications of blood-derived and marrow-derived stem cells for nonmalignant diseases. JAMA 299: 925-936, 2008.
12. Frenette PS, Pinho S, Lucas D and Scheiermann C: Mesenchymal stem cell: Keystone of the hematopoietic stem cell niche and a stepping-stone for regenerative medicine. Annu Rev Immunol 31: 285-316, 2013.
13. Oswald J, Boxberger S, Jørgensen B, Feldmann S, Ehninger G, Bornhäuser M and Werner C: Mesenchymal stem cells can be differentiated into endothelial cells in vitro. Stem Cells 22: 377-384, 2004.
14. Reyes M, Dudek A, Jahagirdar B, Koodie L, Marker PH and Verfaillie CM: Origin of endothelial progenitors in human post-natal bone marrow. J Clin Invest 109: 337-346, 2002.
15. Wang D, Liu Y, Zhong G, Wang Y, Zhang T, Zhao Z, Yan X and Liu Q: Compatibility of Tanshinone IIA and Astragaloside IV in attenuating hypoxia-induced cardiomyocytes injury. J Ethnopharmacol 204: 67-76, 2017.

16. Xie J, Wang H, Song T, Wang Z, Li F, Ma J, Chen J, Nan Y, Yi H and Wang W: Tanshinone IIA and Astragaloside IV promote the migration of mesenchymal stem cells by up-regulation of CXCR4. Protoplasma 250: 521-530, 2013.
17. Wang S, Chen J, Fu Y and Chen X: Promotion of Astragaloside IV for EA-hy926 cell proliferation and angiogenic activity via ERK1/2 pathway. J Nanosci Nanotechnol 15: 4239-4244, 2015.
18. Tong Y, Xu W, Han H, Chen Y, Yang J, Qiao H, Hong D, Wu Y and Zhou C: Tanshinone IIA increases recruitment of bone marrow mesenchymal stem cells to infarct region via up-regulating stromal cell-derived factor-1/CXC chemokine receptor 4 axis in a myocardial ischemia model. Phytomedicine 18: 443-450, 2011.
19. Leybaert L, Lampe PD, Dhein S, Kwak BR, Ferdinandy P, Beyer EC, Laird DW, Naus CC, Green CR and Schulz R: Connexins in cardiovascular and neurovascular health and disease: Pharmacological implications. Pharmacol Rev 69: 396-478, 2017.
20. Malassiné A and Cronier L: Involvement of gap junctions in placental functions and development. Biochim Biophys Acta 1719: 117-124, 2005.
21. Cronier L, Bastide B, Defamie N, Niger C, Pointis G, Gasc JM and Malassiné A: Involvement of gap junctional communication and connexin expression in trophoblast differentiation of the human placenta. Histol Histopathol 16: 285-295, 2001.
22. Yamasaki H, Krutovskikh V, Mesnil M, Columbano A, Tsuda H and Ito N: Gap junctional intercellular communication and cell proliferation during rat liver carcinogenesis. Environ Health Perspect 101 (Suppl 5): S191-S197, 1993.
23. El-Sabban ME, Abi-Mosleh LF and Talhouk RS: Developmental regulation of gap junctions and their role in mammary epithelial cell differentiation. J Mammary Gland Biol Neoplasia 8: 463-473, 2003.
24. Simon AM and McWhorter AR: Decreased intercellular dye-transfer and downregulation of non-ablated connexins in aortic endothelium deficient in connexin37 or connexin40. J Cell Sci 116: 2223-2236, 2003.
25. Alonso F, Domingos-Pereira S, Le Gal L, Derré L, Meda P, Jichlinski P, Nardelli-Haefliger D and Haefliger JA: Targeting endothelial connexin40 inhibits tumor growth by reducing angiogenesis and improving vessel perfusion. Oncotarget 7: 14015-14028, 2016.
26. Gärtner C, Ziegelhöffer B, Kostelka M, Stepan H, Mohr F and Dhein S: Knock-down of endothelial connexins impairs angiogenesis. Pharmacol Res 65: 347-357, 2012.
27. Walker DL, Vacha SJ, Kirby ML and Lo CW: Connexin43 deficiency causes dysregulation of coronary vasculogenesis. Dev Biol 284: 479-498, 2005.
28. Zanotti L, Angioni R, Calì B, Soldani C, Ploia C, Moalli F, Gargesha M, D'Amico G, Elliman S, Tedeschi G, et al: Mouse mesenchymal stem cells inhibit high endothelial cell activation and lymphocyte homing to lymph nodes by releasing TIMP-1. Leukemia 30: 1143-1154, 2016.
29. Pittenger MF, Mackay AM, Beck SC, Jaiswal RK, Douglas R, Mosca JD, Moorman MA, Simonetti DW, Craig S and Marshak DR: Multilineage potential of adult human mesenchymal stem cells. Science 284: 143-147, 1999.
30. Ai WJ, Li J, Lin SM, Li W, Liu CZ and Lv WM: R-Smad signaling-mediated VEGF expression coordinately regulates endothelial cell differentiation of rat mesenchymal stem cells. Stem Cells Dev 24: 1320-1331, 2015.
31. Shi H, Li Y, Feng G, Li L, Fang R, Wang Z, Qu J, Ding P, Zhang X and Ye L: The oncoprotein HBXIP up-regulates FGF4 through activating transcriptional factor Sp1 to promote the migration of breast cancer cells. Biochem Biophys Res Commun 471: 89-94, 2016.
32. Livak KJ and Schmittgen TD: Analysis of relative gene expression data using real-time quantitative PCR and the 2(-Delta Delta C(T)) method. Methods 25: 402-408, 2001.
33. Wang DG, Zhang FX, Chen ML, Zhu HJ, Yang B and Cao KJ: Cx43 in mesenchymal stem cells promotes angiogenesis of the infarcted heart independent of gap junctions. Mol Med Rep 9: 1095-1102, 2014.
34. Michela P, Velia V, Aldo P and Ada P: Role of connexin 43 in cardiovascular diseases. Eur J Pharmacol 768: 71-76, 2015.
35. Li X, Chen YY, Wang XM, Gao K, Gao YZ, Cao J, Zhang ZL, Lei J, Jin ZY and Wang YN: Image-guided stem cells with functionalized self-assembling peptide nanofibers for treatment of acute myocardial infarction in a mouse model. Am J Transl Res 9: 3723-3731, 2017.
36. Chou S, Lin S, Kuo W, Pai P, Lin JY, Lai CH, Kuo CH, Lin KH, Tsai FJ and Huang CY: Mesenchymal stem cell insights: Prospects in cardiovascular therapy. Cell Transplant 23: 513-529, 2014.
37. Wassef MA, Fouad H, Sabry D, Afifi N, Abbas AM, Mostafa W and Ahmed SH: Therapeutic efficacy of differentiated versus undifferentiated mesenchymal stem cells in experimental type I diabetes in rat. Biochem Biophys Rep 5: 468-475, 2016.
38. Gnecchi M, Zhang Z, Ni A and Dzau VJ: Paracrine mechanisms in adult stem cell signaling and therapy. Circ Res 103: 1204-1219, 2008.
39. Wang W, Wang ZR, Zhang JZ, Li J, Li JC and Shi CH: Serum with Qidantongmai induce differentiation of rat mesenchymal stem cells into endothelial cells in vitro. Prog Modren Biomed 6: 20-21, 2006 (In Chinese).
40. Leu YW, Chu PY, Chen CM, Yeh KT, Liu YM, Lee YH, Kuo ST and Hsiao SH: Early life ethanol exposure causes long-lasting disturbances in rat mesenchymal stem cells via epigenetic modifications. Biochem Biophys Res Commun 453: 338-344, 2014.
41. Li H, He J, Yu H, Green CR and Chang J: Bioglass promotes wound healing by affecting gap junction connexin 43 mediated endothelial cell behavior. Biomaterials 84: 64-75, 2016.
42. Hirschi KK, Burt JM, Hirschi KD and Dai C: Gap junction communication mediates transforming growth factor-beta activation and endothelial-induced mural cell differentiation. Circ Res 93: 429-437, 2003.
43. Bergers G and Song S: The role of pericytes in blood-vessel formation and maintenance. Neuro Oncol 7: 452-464, 2005.